



# Analysis of Forced Convection on Velocity Profile and Temperature Distribution in a Square Enclosure

Rasid Okeyo Odira <sup>a\*</sup>, Johana Kibet Sigey <sup>a</sup>,  
Jeconia Okelo Abonyo <sup>a</sup> and Bulinda M. Vincent <sup>b</sup>

<sup>a</sup> Department of Pure and Applied Mathematics, Jomo Kenyatta University of Agriculture and Technology, Kenya.

<sup>b</sup> Department of Mathematics and Actuarial Science, Kisii University, Kenya.

## Authors' contributions

*This work was carried out in collaboration among all authors. All authors read and approved the final manuscript.*

## Article Information

DOI: 10.9734/JAMCS/2023/v38i101830

## Open Peer Review History:

This journal follows the Advanced Open Peer Review policy. Identity of the Reviewers, Editor(s) and additional Reviewers, peer review comments, different versions of the manuscript, comments of the editors, etc are available here: <https://www.sdiarticle5.com/review-history/107554>

**Received: 06/08/2023**

**Accepted: 13/10/2023**

**Published: 20/10/2023**

**Original Research Article**

## Abstract

The research project focused on a forced convection in a three dimensional square enclosure with a heater placed at the center of the room, a window on one of the adjacent walls of the enclosure and two fans fixed along the other wall. To carry out analyzing of the flow and heat transfer rate, a set of non-dimensionalized equations governing Newtonian fluid and boundary conditions were discussed. These equations with boundary conditions are discretized using central difference approximation method. The results obtained from finite difference equations (FDE) were then solved using MATLAB simulation software. The results found reveal that, both the horizontal and vertical velocity profiles are increased by Richardson number, and Reynolds number. Also Eckert number together with dimensionless heat absorption coefficient leads to an increase in the temperature distribution. The obtained results are presented in graphs and tables to show temperature distribution and velocity profile in the room with both physical and scientific explanations.

\*Corresponding author: Email: rashidokeyo701@gmail.com;

**Keywords:** Square enclosure; finite difference equations (fde); matlab simulation software; high velocity fluid; thermal resistance.

## Nomenclature and Abbreviation

$\alpha$	: Thermal diffusivity;
$\rho$	: Density ( $\text{kg/m}^3$ );
$T$	: Thermodynamic temperature in Kelvin (K);
$P$	: Static pressure ( $\text{n/m}^2$ );
$t$	: Time in seconds (m/s);
$Q_h$	: Heat flux;
$h_c$	: Heat transfer coefficient;
$T_s$	: Surface temperature (K);
$T_f$	: Fluid temperature (K);
$\rho$	: Denotes thermodynamic pressure;
$\mu$	: Kinematic viscosity;
$g$	: Gravitational acceleration;
$\beta$	: Thermal expansion coefficient;
$U.W.T$	: Uniform Wall Temperature;
$UHF$	: Uniform Heat flux;
$FDM$	: Finite Difference Method;
$MATLAB$	: Matrix Laboratory;
$3D$	: Three dimensions.

## 1 Introduction

### 1.1 Background of the study

“Heat transfer by forced convection makes use a fan or a blower to provide high velocity fluid. The high velocity fluid in the fluid results in a decrease thermal resistance across the boundary from the fluid to the heated surfaces. This intern will increase the amount of heat that is carried away by the fluid. In most electronic devices fans have been used to enhance heat exchange within the system of those devices. The device does dissipate heat while in operation and therefore require cooling system that hastens fluid mixing. Scientific fields such as civil engineering, structures are developed while considering proper air circulation within the structures. Convictional heaters are fixed in the structures to help temperature regulation and air flow within the structures for proper functioning. Convection is the process where heat is transferred in the fluids by movement of the currents from one region to another. This process occurs between the surfaces of the moving fluids with different temperatures. Motion of the fluid is influenced by the following factors: heat transfer, but when the velocity is higher, the rate of heat transfer is also higher. The process of convection of heat depends on specific heat, density of the fluid and thermal conductivity. Velocity of the fluid is assumed to be zero at the wall” [1].

In forced convection, heat transfer involves motion of the particle and conduction of the heat within the body. The process of forced convection corresponds to configuration where the flow is accelerated by external factors or devices such as pumps and fans that dominates buoyancy effects. In this case the flow regime can be characterized, similarly to isothermal flow using the Reynolds number as the indicator. Reynolds number is the ratio of the inertia to viscous forces.

Sigey et al. [1] studied “buoyancy driven free convection turbulent heat transfer in an enclosure. They investigated a three dimensional enclosure containing a convectional heater built into one wall having a window in same wall. The heater is located below the window and the other remaining wall insulated. The results were that three regions a cold upper region, a hot region in the area between and a warm lower region”.

Okewa et al. [2] studied “forced convection in a three dimensional rectangular enclosure with heaters placed on the opposite wall on the y-z planes and two windows on the adjacent opposite walls on x-z planes and one fan centrally fixed at the top (ceiling) x-y plane. The fan was set to rotate with varying speed. Results obtained

showed that temperature increases with increase in room depth and as the fan speed increases, temperature increases with increase in room depth at a lower rate. It was also found that the rate of increase in temperature is higher with increase in the room's depth. At any particular room depth, temperature was higher at lower Reynolds number and lower at high Reynolds number but lowest velocity when Reynolds number is high and highest at low Reynolds number. The temperatures within the room were lower when the fan speed is increased. The velocity of air within the room decreases with decrease in rooms depth and decreases at lower Reynolds number”.

Onchaga et al. (2012) studied “turbulent convection of heat with localized heating and cooling and on adjacent vertical wall enclosed on a cubic enclosure. A convectional heater was placed on the Centre bottom surface with two windows placed on adjacent vertical walls and temperature of the heater was varied. The governing equations with the boundary conditions were described using three-point central and forward difference approximations. From the graphs of velocity profile and temperature distribution, it was noted that the heater records high temperatures but it decreased as it moved upwards. This was due to the warm air which gained energy hence rising. At the window region least temperature was recorded hence the fluid descends moved in the direction of the heater”.

Rehena et al. (2013) investigated “forced convection heat transfer phenomenon in a two dimensional horizontal channel having an open cavity with porous medium. A non uniform heat flux was considered to be located on the bottom surface cavity. The three different heating modes at the bottom, the rest of the surfaces were considered to be perfectly adiabatic. The physical domain was filled with water based nano fluid. Fluid entered from left and exits from right. Results showed that increasing Prandtl causes the enhancement of heat transfer rate”.

Momanyi et al. [4] studied “effects of a forced convection on a temperature distribution and velocity profile in a rectangular enclosure with heaters fitted on opposite walls two windows on the adjacent opposite walls and a fan centrally fixed at the top. The temperature distribution and the velocity profile were studied by varying Prandtl number, Reynolds number and pressure. The result showed that temperature at a given depth decreases with an increase in Reynolds number and increase in Prandtl number. The flow velocity was revealed to be low at high pressure and at high low pressure” [5-7].

Sigey et al, [2] studied “convection in a room with heater and window placed in the same wall. This was done by using a rectangular enclosure. The heater was placed below the window and other parts of the room were insulated. It was noted that heat transfer is higher when the window is wide as Rayleigh number increases” [8].

“Most scholars have studied temperature distribution and velocity profile in an enclosure considering free convection, others have looked at forced convection with various geometry” [1,9,10]. This study looks at analysis of forced convection on velocity profiles and temperature distribution in a square enclosed room considering a heater placed at the center, fans fitted at the adjacent wall.

## **2 Methodology**

This chapter discusses the equations that govern the flow of fluids with reference to air in a square room. By considering the nature of the problem the equations are presented in two dimensions in horizontal and vertical directions.

### **2.1 Conservation equation**

“The viscous incompressible fluid flow and the temperature distribution inside the square room are described by the momentum and energy equations. Systems of Navier-stokes and energy partial differential equations with appropriate boundary conditions governing our problem are solved using a Finite Difference Method. The fluid flow is expressed theoretically by momentum and energy equations under the assumption that the fluid flow is steady, laminar, incompressible and two-dimensional” [1].

## 2.2 Computational procedure

In this study a three point central Finite Difference numerical scheme is developed. This method is used to solve the momentum equation and energy equation. “The method obtains a finite system of linear or nonlinear algebraic equations from the momentum and energy equations Partial Differential Equation by discretizing the given equation and coming up with the numerical schemes analogues to the equation, in this case the momentum and energy equations. We solve the equations subject to the given boundary conditions. MATLAB software is used to find solution values in this study” [1].

## 2.3 The governing equations

“Thermo physical properties of the fluid in the flow model are assumed to be constant except the density variations causing body force term in the Momentum Equation. The Boussinesq approximation is invoked for the fluid properties to relative density changes to temperature changes, and to couple in this way the temperature field to the flow field. The governing equations for the flow using conservation of mass, momentum and energy are discussed as follows” [1].

## 2.4 Momentum conservation equations

The equation is derived from the Newton’s second law of motion which states that, the sum of the body and surface forces acting on a system is equal to the rate of change of linear momentum of the system. For forced convection the following momentum equation holds

$$\rho u \frac{\partial u}{\partial x} + \rho v \frac{\partial u}{\partial y} = -\frac{\partial p}{\partial x} + \mu \left( \frac{\partial^2 u}{\partial x^2} + \frac{\partial^2 u}{\partial y^2} \right) \quad (1)$$

$$\rho u \frac{\partial v}{\partial x} + \rho v \frac{\partial v}{\partial y} = -\frac{\partial p}{\partial y} + \mu \left( \frac{\partial^2 v}{\partial x^2} + \frac{\partial^2 v}{\partial y^2} \right) + g\beta(T - T_o) \quad (2)$$

## 2.5 Energy conservation equation

The energy equation is derived from the first law of thermodynamics which states that the rate of energy increase in a system is equated to the heat added to the system and work done on the system. From Currie (1974), assuming no external heat source, the energy equation is written as

$$\rho c_p u \frac{\partial T}{\partial x} + \rho c_p v \frac{\partial T}{\partial y} = \alpha \left( \frac{\partial^2 T}{\partial x^2} + \frac{\partial^2 T}{\partial y^2} \right) + \mu\Phi \quad (3)$$

## 2.6 Solution methods

The momentum and energy equations are non-dimensionalised to reduce the complexity of the problem. Dimensional analysis makes the equations more concise from the physical relationship. This process reduces the number of independent variables that defines the problem. Using the following dimensionless variables;

$$X = \frac{x}{L}, Y = \frac{y}{L}, U = \frac{u}{u_o}, V = \frac{v}{v_o}, P = \frac{p}{\rho u_o^2}, \theta = \frac{T - T_o}{T_1 - T_o} \quad (4)$$

## 2.7 Momentum equation along the horizontal axis

By considering the x-component, Navier-Stoke's equations for the horizontal velocity profile. Substituting the non-dimensional variables in (4) into (1) we get;

$$\frac{\rho u^2}{L} U \frac{\partial u}{\partial x} + \frac{\rho u^2}{L} V \frac{\partial u}{\partial y} = -\frac{\rho u^2}{L} \frac{\partial p}{\partial x} + \frac{\mu u}{L^2} \left( \frac{\partial^2 u}{\partial x^2} + \frac{\partial^2 u}{\partial y^2} \right) \quad (5)$$

Multiplying (4) by  $\frac{L}{\rho \mu^2}$  we get

$$u \frac{\partial u}{\partial x} + v \frac{\partial u}{\partial y} = -\frac{\partial P}{\partial x} + \frac{\mu}{\rho u_o L} \left( \frac{\partial^2 u}{\partial x^2} + \frac{\partial^2 u}{\partial y^2} \right) \quad (6)$$

But,  $Re = \frac{\rho u_o L}{\mu}$ , hence the non-dimensional form of the x-component of the Navier-Stoke's equation become

$$U \frac{\partial u}{\partial x} + V \frac{\partial u}{\partial y} = -\frac{\partial p}{\partial x} + \frac{1}{Re} \left( \frac{\partial^2 u}{\partial x^2} + \frac{\partial^2 u}{\partial y^2} \right) \quad (7)$$

## 2.8 Momentum equation along the vertical axis

Considering the y-component, Navier-Stoke's equations for the vertical velocity profile. Substituting the non-dimensional variables in (4) into (2) we get;

$$U \frac{\partial v}{\partial x} + V \frac{\partial v}{\partial y} = -\frac{\partial p}{\partial x} + \frac{1}{Re} \left( \frac{\partial^2 v}{\partial x^2} + \frac{\partial^2 v}{\partial y^2} \right) + \frac{Gr}{Re^2} \theta \quad (8)$$

Richardson number is defined as;

$$Ri = \frac{Gr}{Re^2}; \text{ where Grashof number and Reynolds number are defined as;}$$

$$Gr = \frac{g\beta(T_1 - T_o)L^3}{\mu^2}, Re = \frac{u_o L}{\mu}$$

Thus equation (8) become

$$U \frac{\partial v}{\partial x} + V \frac{\partial v}{\partial y} = -\frac{\partial P}{\partial y} + \frac{1}{Re} \left( \frac{\partial^2 v}{\partial x^2} + \frac{\partial^2 v}{\partial y^2} \right) + Ri\theta \quad (9)$$

## 2.9 Dimensionalization of energy equation

Considering the energy equation (3) and substituting the non-dimensional variables in (4) into (3) we get

$$\frac{\rho c_p u_o (T_1 - T_o)}{L} \left( U \frac{\partial \theta}{\partial x} + V \frac{\partial \theta}{\partial y} \right) = \alpha \frac{(T_1 - T_o)}{L^2} \left( \frac{\partial^2 \theta}{\partial x^2} + \frac{\partial^2 \theta}{\partial y^2} \right) + \frac{\mu u_o^2}{L^2} \Phi \quad (10)$$

Simplify equation (10) we get

$$U \frac{\partial \theta}{\partial x} + V \frac{\partial \theta}{\partial y} = \frac{\alpha}{\rho c_p u_o L} \left( \frac{\partial^2 \theta}{\partial x^2} + \frac{\partial^2 \theta}{\partial y^2} \right) + \frac{\mu u_o^2}{\rho c_p L (T_1 - T_o)} \Phi \quad (11)$$

At low velocities, viscous dissipation is negligible.

$$\text{But } \frac{\alpha}{\rho c_p u_o L} = \frac{\alpha}{\rho c_p u_o L} \left( \frac{\mu}{\mu} \right) = \left( \frac{\alpha}{\mu c_p} \right) \left( \frac{\mu}{\rho u_o L} \right)$$

$$\text{And } \text{Pr} = \frac{\mu c_p}{\alpha}, \text{Re} = \frac{\rho u_o L}{\mu}, E_c = \frac{\mu u_o^2}{\rho c_p L (T_1 - T_o)} \quad (12)$$

Equation (11) therefore becomes

Where  $E_c$  is the Eckert number and  $\phi$  is the heat generation coefficient.

## 2.10 Discretization of governing equations using mesh grid

We discretize the momentum and energy equations and form three point central difference schemes for each equation which we eventually solve using the finite difference method.

### 2.10.1 Horizontal Velocity Profile

Our equation (7) is discretized to show the effects of Re for horizontal velocity profiles. Using a central difference numerical scheme,  $u_x$ ,  $u_y$ ,  $u_{xx}$  and  $u_{yy}$  is replaced by three point Central difference approximation. When these approximations are substituted into equation (3.7), we get

$$U \frac{U_{i+1,j} - U_{i-1,j}}{2\Delta x} + V \frac{U_{i,j+1} - U_{i,j-1}}{2\Delta y} = - \left( \frac{P_{i+1,j} - P_{i-1,j}}{2\Delta x} \right) + \frac{1}{\text{Re}} \left[ \frac{U_{i+1,j} - 2U_{i,j} + U_{i-1,j}}{(\Delta x)^2} + \frac{U_{i,j+1} - 2U_{i,j} + U_{i,j-1}}{(\Delta y)^2} \right] \quad (13)$$

We investigate the effect of Re, on the fluid velocity. Taking  $\Delta x = \Delta y = \frac{1}{4} = 0.25$ , and  $V = U = 1$ , and multiply by  $16\text{Re}\Delta x$  we get the central difference scheme

$$(8\text{Re}-1)U_{i+1,j} + 4U_{i,j} - (8\text{Re}+1)U_{i-1,j} = (1-8\text{Re})U_{i,j+1} + (8\text{Re}+1)U_{i,j-1} + 8\text{Re}P_{i+1,j} - 8\text{Re}P_{i-1,j} \quad (14)$$

Taking and  $i=1,2,3,\dots,6$  and  $j=1$  we form the following systems of linear algebraic equations

$$\begin{aligned}
 (8\text{Re}-1)U_{2,1} + 4U_{1,1} - (8\text{Re}+1)U_{0,1} &= -8\text{Re} P_{2,1} + 8\text{Re} P_{0,1} + (1-8\text{Re})U_{1,2} + (8\text{Re}+1)U_{1,0} \\
 (8\text{Re}-1)U_{3,1} + 4U_{2,1} - (8\text{Re}+1)U_{1,1} &= -8\text{Re} P_{3,1} + 8\text{Re} P_{1,1} + (1-8\text{Re})U_{2,2} + (8\text{Re}+1)U_{2,0} \\
 (8\text{Re}-1)U_{4,1} + 4U_{3,1} - (8\text{Re}+1)U_{2,1} &= -8\text{Re} P_{4,1} + 8\text{Re} P_{2,1} + (1-8\text{Re})U_{3,2} + (8\text{Re}+1)U_{3,0} \\
 (8\text{Re}-1)U_{5,1} + 4U_{4,1} + (8\text{Re}+1)U_{3,1} &= -8\text{Re} P_{5,1} + 8\text{Re} P_{3,1} + (1-8\text{Re})U_{4,2} + (8\text{Re}+1)U_{4,0} \\
 (8\text{Re}-1)U_{6,1} + 4U_{5,1} + (8\text{Re}+1)U_{4,1} &= -8\text{Re} P_{6,1} + 8\text{Re} P_{4,1} + (1-8\text{Re})U_{5,2} + (8\text{Re}+1)U_{5,0} \\
 (8\text{Re}-1)U_{7,1} + 4U_{6,1} + (8\text{Re}+1)U_{5,1} &= -8\text{Re} P_{7,1} + 8\text{Re} P_{5,1} + (1-8\text{Re})U_{6,2} + (8\text{Re}+1)U_{6,0}
 \end{aligned} \tag{15}$$

By solving the matrix equation above, we get the solutions for varying values of Reynold’s number to be =500,550 and 600 as shown in Table 1 in chapter 4.

### 2.10.2 Vertical velocity profile equation

Equation (9) was discretized to study the effects of Re and Ri for vertical velocity profiles. Using a Hybrid difference numerical scheme,  $V_x$ ,  $V_y$ ,  $V_{xx}$  and  $V_{yy}$  are replaced by three point central difference approximation. When these approximations are substituted into equation (3.7), we get

$$U \frac{V_{i+1,j} - V_{i,j}}{2\Delta x} + V \frac{V_{i,j+1} - V_{i,j-1}}{2\Delta y} = -\frac{P_{i,j+1} - P_{i,j-1}}{2\Delta y} + \frac{1}{\text{Re}} \left[ \frac{V_{i+1,j} - 2V_{i,j} + V_{i-1,j}}{(\Delta x)^2} + \frac{V_{i,j+1} - 2V_{i,j} + V_{i,j-1}}{(\Delta y)^2} \right] + Ri\theta \tag{16}$$

By investigate the effect of Re and Ri on the fluid velocity. Taking  $\theta = 10$ ,  $\Delta x = \Delta y = 0.25$ , and  $V = U = 1$  into (16), we get the scheme

$$(1-8\text{Re})V_{i,j+1} - 4V_{i,j} + (8\text{Re}+1)V_{i,j-1} = 8\text{Re} P_{i,j-1} - 8\text{Re} P_{i,j+1} + (1-8\text{Re})V_{i+1,j} + (8\text{Re}+1)V_{i-1,j} + Ri\theta \tag{17}$$

As we chose  $i = 1$  and  $j = 1, 2, \dots, 6$ , we form the following systems of linear algebraic equations

$$\begin{aligned}
 (1-8\text{Re})V_{1,2} - 4V_{1,1} + (8\text{Re}+1)V_{1,0} &= 8\text{Re} P_{1,0} - 8\text{Re} P_{1,2} + (1-8\text{Re})V_{2,1} + (8\text{Re}+1)V_{0,1} + Ri\theta \\
 (1-8\text{Re})V_{1,3} - 4V_{1,2} + (8\text{Re}+1)V_{1,1} &= 8\text{Re} P_{1,1} - 8\text{Re} P_{1,3} + (1-8\text{Re})V_{2,2} + (8\text{Re}+1)V_{0,2} + Ri\theta \\
 (1-8\text{Re})V_{1,4} - 4V_{1,3} + (8\text{Re}+1)V_{1,2} &= 8\text{Re} P_{1,2} - 8\text{Re} P_{1,4} + (1-8\text{Re})V_{2,3} + (8\text{Re}+1)V_{0,3} + Ri\theta \\
 (1-8\text{Re})V_{1,5} - 4V_{1,4} + (8\text{Re}+1)V_{1,3} &= 8\text{Re} P_{1,3} - 8\text{Re} P_{1,5} + (1-8\text{Re})V_{2,4} + (8\text{Re}+1)V_{0,4} + Ri\theta \\
 (1-8\text{Re})V_{1,6} - 4V_{1,5} + (8\text{Re}+1)V_{1,4} &= 8\text{Re} P_{1,4} - 8\text{Re} P_{1,6} + (1-8\text{Re})V_{2,5} + (8\text{Re}+1)V_{0,5} + Ri\theta \\
 (1-8\text{Re})V_{1,7} - 4V_{1,6} + (8\text{Re}+1)V_{1,5} &= 8\text{Re} P_{1,5} - 8\text{Re} P_{1,7} + (1-8\text{Re})V_{2,6} + (8\text{Re}+1)V_{0,6} + Ri\theta
 \end{aligned} \tag{18}$$

By Solving the matrix equation (19) above, we get the solutions for varying values of Ri and Re with  $\theta = 10^\circ$  we get results

### 2.11 Temperature distribution

The energy Equation (12) is discretized to study the effects of Re for temperature profiles. A ir in the room is considered to have fixed Prandtl number 0.71. Using a three point central numerical scheme, we get

$$\frac{\theta_{i,j+1} - \theta_{i,j}}{\Delta t} + U \frac{\theta_{i+1,j} - \theta_{i-1,j}}{2\Delta x} + V \frac{\theta_{i,j+1} - \theta_{i,j-1}}{2\Delta y} = \frac{1}{\text{Pr Re}} \left[ \frac{\theta_{i+1,j} - 2\theta_{i,j} + \theta_{i-1,j}}{(\Delta x)^2} + \frac{\theta_{i,j+1} - 2\theta_{i,j} + \theta_{i,j-1}}{(\Delta y)^2} \right] + E_c \Phi \tag{20}$$

By investigating the effect of Re, on the fluid velocity. We take Pr = 0.71 since the fluid is air. Taking i = 1, j = 1,2,...,6, Δt = 0.1, Δx = Δy = 0.25, Re=100 and V=1, U=1, we get the scheme

$$(1-67.2\text{Re})\theta_{i,j+1}^n + (11.2\text{Re}-4)\theta_{i,j}^n + (8\text{Re}+1)\theta_{i,j-1}^n = (56\text{Re}-1)\theta_{i+1,j}^n - (56\text{Re}+1)\theta_{i-1,j}^n - E_c\Phi \quad (21)$$

As we chose i=1 and j=1,2,3...6 we form the following systems of linear algebraic equations

$$\begin{aligned} (1-56\text{Re})\theta_{1,2}^0 + (11.2\text{Re}-4)\theta_{1,1}^0 + (8\text{Re}+1)\theta_{1,0}^0 &= (56\text{Re}-1)\theta_{2,1}^0 - (56\text{Re}+1)\theta_{0,1}^0 + 11.2\theta_{1,1}^1 - E_c\Phi \\ (1-56\text{Re})\theta_{1,3}^0 + (11.2\text{Re}-4)\theta_{1,2}^0 + (8\text{Re}+1)\theta_{1,1}^0 &= (56\text{Re}-1)\theta_{2,2}^0 - (56\text{Re}+1)\theta_{0,2}^0 + 11.2\theta_{1,2}^1 - E_c\Phi \\ (1-56\text{Re})\theta_{1,4}^0 + (11.2\text{Re}-4)\theta_{1,3}^0 + (8\text{Re}+1)\theta_{1,2}^0 &= (56\text{Re}-1)\theta_{2,3}^0 - (56\text{Re}+1)\theta_{0,3}^0 + 11.2\theta_{1,3}^1 - E_c\Phi \\ (1-56\text{Re})\theta_{1,5}^0 + (11.2\text{Re}-4)\theta_{1,4}^0 + (8\text{Re}+1)\theta_{1,3}^0 &= (56\text{Re}-1)\theta_{2,4}^0 - (56\text{Re}+1)\theta_{0,4}^0 + 11.2\theta_{1,4}^1 - E_c\Phi \\ (1-56\text{Re})\theta_{1,6}^0 + (11.2\text{Re}-4)\theta_{1,5}^0 + (8\text{Re}+1)\theta_{1,4}^0 &= (56\text{Re}-1)\theta_{2,5}^0 - (56\text{Re}+1)\theta_{0,5}^0 + 11.2\theta_{1,5}^1 - E_c\Phi \\ (1-56\text{Re})\theta_{1,7}^0 + (11.2\text{Re}-4)\theta_{1,6}^0 + (8\text{Re}+1)\theta_{1,5}^0 &= (56\text{Re}-1)\theta_{2,6}^0 - (56\text{Re}+1)\theta_{0,6}^0 + 11.2\theta_{1,6}^1 - E_c\Phi \end{aligned} \quad (22)$$

### 3 Results and Discussion

The simulation results given focus on the effects of the Reynolds number Re, Richardson number Ri, Eckert number E<sub>c</sub> and heat absorption coefficient φ, on velocity profile and temperature distribution respectively.

#### 3.1 Effect of reynolds number horizontal velocity profile

As we solve equation (16) using MATLAB and get the results of the effects of Reynolds number on horizontal velocity profile

**Table 1. Value of horizontal velocity profile for varying Reynolds number**

Reynolds number	Length of square room				
	0	1	2	3	4
<b>Re = 500</b>	667.2576	1.3354	667.583	0.6674723	667.916
<b>Re = 550</b>	733.917	1.333788	734.249913	0.6671978	734.58366
<b>Re = 600</b>	800.583621	1.33375	800.9196	0.6671529	801.2502

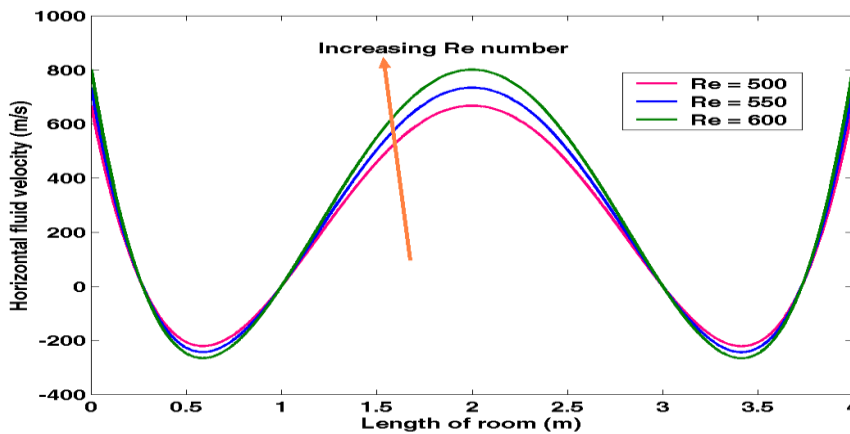


**Fig. 1. A graph of horizontal velocity against Length of room at varying Reynolds' number**



Effect of Reynolds number on horizontal velocity can be observed from Fig. 1. Increase in Reynolds number leads to increases in the horizontal velocity. An increase in fluid Reynolds number leads to increases in the vertical velocity profile. As we increase the length of the enclosure, the vertical velocity decreases at the middle of room except near the walls. Viscous forces became dominant. As the value of Re increased, the inertia forces dominated over the viscous force and the velocity increased.

### 3.2 Effect of Richardson number on vertical velocity profile

By solving equation (19) using MATLAB and get the results of the effects of Richardson number on vertical velocity profile.

**Table 2. Value of vertical velocity profile for varying Richardson numbers**

Richardson number	Length of room				
	0	1	2	3	4
<b>Ri = 5.0</b>	1211.235	0.001263105	1212.75	0.001263456	1241.266
<b>Ri = 6.0</b>	1313.731	0.001265709	1315.25	0.00126606	1316.77
<b>Ri = 7.0</b>	1416.228	0.0012683313	1417.75	0.001268665	1419.273

Effect of Richardson number on vertical velocity can be observed from figure 2. Increase in Richardson numbers leads to increases in the vertical velocity profile. As we vary Richardson number, the vertical velocity decreases as the length of the enclosure increases from the top of room heating downwards. Fluid velocities are relatively lower near the walls of the room but higher at the middle. This is due to the fact that near the ground of room height enclosure, kinetic energy increases leading to an increase in fluid vertical velocity. On the upper side of the room, the kinetic energy of the fluid particles starts to decreases resulting to a decrease in vertical fluid velocity profile.

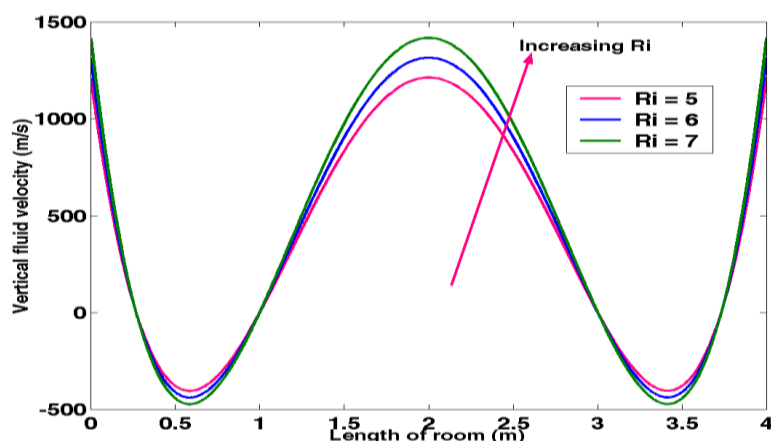


**Fig. 2. A graph of vertical velocity against Length of room at varying Richardson numbers**

### 3.3 Effect of Reynolds number on vertical velocity profile

We solve equation (19) using MATLAB and get the results of the effects of Reynolds number on vertical velocity profile.

**Table 3. Value of vertical velocity profile for varying Reynolds number**

Reynolds number	Length of room				
	0	1	2	3	4
<b>Re = 500</b>	337.7521	0.6751667	-336.9087	0.6744918	338.0895
<b>Re = 550</b>	537.0853	0.674394	-370.2428	0.7567812	538.4223
<b>Re = 600</b>	737.235	0.6763105	-416.75	0.75663456	738.266

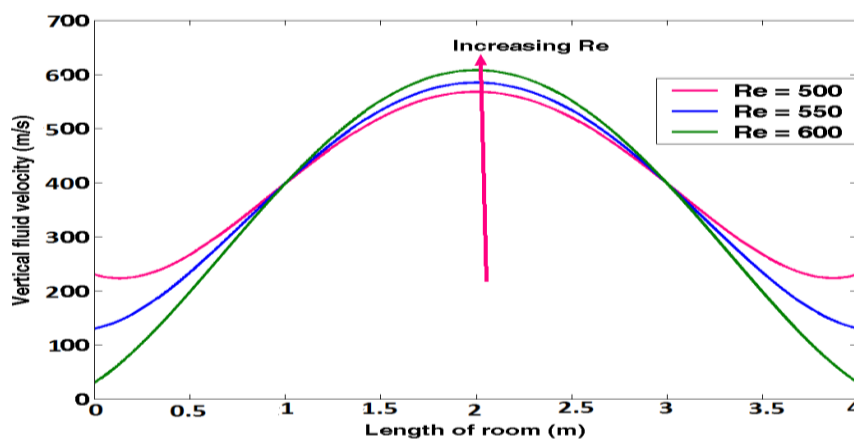


Fig. 3. A graph of vertical velocity against Length of room at varying Reynolds number

Effect of Reynolds number on vertical velocity profile can be observed from figure 3. An increase in fluid Reynolds number leads to increases in the vertical velocity profile. As the length of the enclosure increased, the vertical velocity increased at the middle height of room except near ground and at the top. The viscous forces became dominant. As the value of Re increased, the inertia forces dominated over the viscous force and the velocity increased.

### 3.4 Effect of Eckert number on the distribution of temperature

We solve equation (23) using MATLAB and get the results of the effects of Eckert number on temperature distribution.

Table 4. Value of velocity profile for varying Eckert number

Eckert number	Height of room				
	0	1	2	3	4
$E_c = 1.0$	99.3448	18.71209	16.78558	4.884094	2.230255
$E_c = 3.0$	104.40656	23.73379	21.79607	9.887145	7.231649
$E_c = 5.0$	109.46862	28.73547	26.80655	14.890197	12.233042

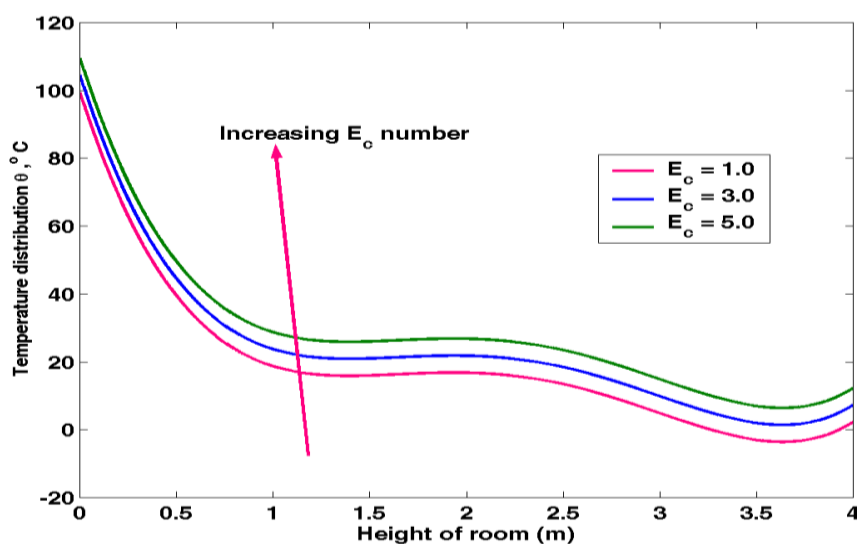


Fig. 4. A graph of temperature distribution against Room Height at varying Eckert number

Effect of Eckert number on temperature distribution can be observed from Fig. 4. Increase in Eckert number leads to increases in the temperature distribution. With an increase in  $Ec$ , the fluid temperature increases in a region just before the bottom of the room and then decreases in the region at the top of the room. Eckert number is a ratio of kinetic energy to the enthalpy. This means that a large Eckert number implies more kinetic energy and reduced temperature difference. Kinetic energy increase and reduced temperature difference implies that more heat transfer and hence the rise in temperature profiles distribution. However kinetic energy reduces as distance increases in a vertical direction whereas thermal energy difference across the boundary layer increases as distance increase in the same direction. This implies that there is more heat generation at the bottom of the room. The result revealed that, an increase in Eckert number leads to increase in temperature.

### 3.5 Effect of heat absorption coefficient on temperature distribution

By solving equation (23) using MATLAB and get the results of the effects of heat absorption coefficient of temperature distribution.

**Table 5. Value of temperature distribution for varying heat absorption coefficient**

Heat absorption coefficient	Height of room				
	0	1	2	3	4
$\phi = 10$	99.3448	18.71209	16.78558	4.884094	2.230255
$\phi = 20$	119.4793	38.73238	36.81142	24.890711	22.246976
$\phi = 30$	129.4702	48.73928	46.81629	34.891225	32.26091

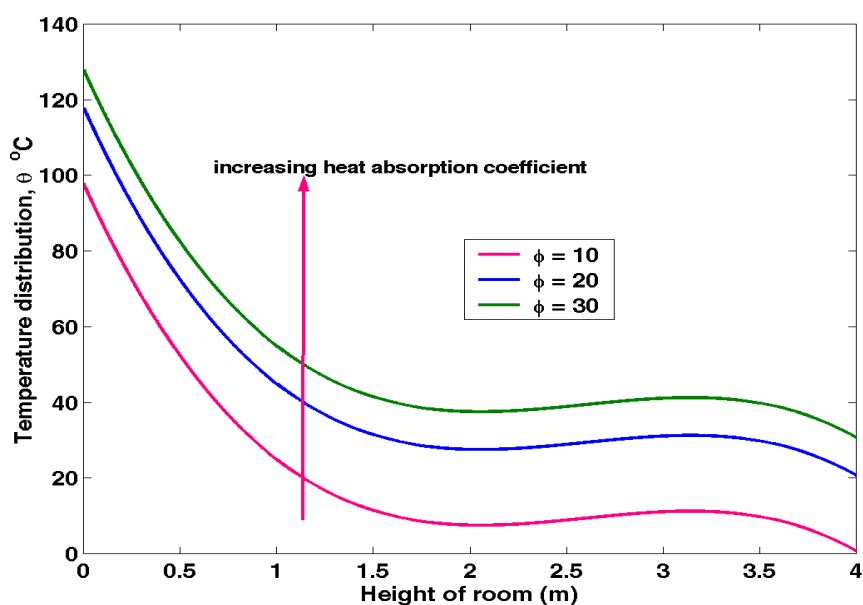


**Fig. 5. A graph of temperature distribution against room Height at varying heat absorption coefficient**

Effect of heat absorption coefficient on temperature distribution can be observed from Fig. 5. Increase in heat absorption coefficient leads to increases in the temperature distribution. It is noticed that as the dimensionless heat absorption coefficient increases, the temperature is found to be decreasing in the boundary layer region. However, the change is not that significant. Further, slightly away from the place the dispersion in the temperature is considerable and thereafter as we move far away from the plate, the effect is found to be decreasing.

## 4 Conclusion and Recommendation

### 4.1 Conclusion

A numerical study performed to analyze forced convection on velocity profile and temperature distribution in a square enclosure. The following outcomes can be written from the study.

- Increase in Reynolds number yields an increase in the horizontal velocity profile.
- As we increase the Richardson numbers, it leads to increases in the vertical velocity profile.
- An increase in fluid Reynolds number leads to increases in the vertical velocity profile.
- Increase in Eckert parameter leads to increases in the temperature distribution.
- It's also noticed that, as the dimensionless heat absorption coefficient increases, the temperature is found to be decreasing

### 4.2 Recommendations of the study

The following areas arise for further analysis and development:

- An extension of this study to factor in a varying magnetic field strength.
- An extension of this study to incorporate buoyancy ratio in fluids which are compressible.
- A study involving MHD both natural and forced convection flow with magnetic field applied along the vertical axis.

## Competing Interests

Authors have declared that no competing interests exist.

## References

- [1] Eva AO. Effect of forced convection on temperature distribution and velocity profile in a rectangular room, *The international Journal of Science & Technology*. 2019;5:22-35.
- [2] Sigey JK, Gatheri F, Kinyanjui M. Buoyancy Driven Free Convection Turbulent Heat Transfer in an Enclosure. *Journal of Agriculture, Science and Technology*. 2011;12(1).
- [3] Okewa JO, Sigey JK, Okelo JA, Giterere K. Effects of Forced Convection on Temperature Distribution and Velocity Profile in a Rectangular Enclosure with Varying Fan Speed, *The International Journal of Science & Technology*. 2017;5:23-32.
- [4] Momanyi JN, Sigey JK, Okello JA, Okwoyo JM. Effect of Forced Convection on Temperature Distribution and Velocity Profile in a Room. *The SIJ Transactions on Computer and Network and Communication Engineering*. 2015;3(3)2321-2403.
- [5] Ghadhimi M, Ghadamian H, Hamidi AA, Fazelpour F, Behghadan MA. Analysis of Free and Forced Convection in Air Flow Windows using Numerical Simulation of Heat Transfer. *International Journals of Energy and Environmental Engineering*. 2012;3:1–10.
- [6] Gikundi A, Awuor K, Karanja S. A numerical study of turbulent natural convection in a rectangular enclosure heated from below. *German Journal of Advanced Scientific Research (GJASR)*. 2020;3(4).
- [7] Mairura EO, Sigey JK, Okello JA, Okwoyo JM. Natural Convection with Localized Heating and Cooling on the Opposite Walls in an Enclosure. *The SIJ Transaction on Computers and Network Communication Engineering*. 2013;1(4):72-78.

- [8] Salleh MZ. Numerical Solution of Forced Convective Boundary Condition Layer Flow on an Horizontal Circular Cylinder with Newtonian Heating,” Malaysian Journal of Mathematical Sciences. 2011;5:162-184.
- [9] Sigey JK. Three-Dimensional Buoyancy Driven Natural Convection in an Enclosure. PhD Thesis, JKUAT, Kenya; 2004.
- [10] Summon S. Combined Free and Forced Convection inside a Two Dimensional Multiple Ventilated Rectangular Enclosure. Asian Research Publishing Network. 2006;1(3):23-35.

---

© 2023 Odira et al.; This is an Open Access article distributed under the terms of the Creative Commons Attribution License (<http://creativecommons.org/licenses/by/4.0>), which permits unrestricted use, distribution, and reproduction in any medium, provided the original work is properly cited.

**Peer-review history:**

The peer review history for this paper can be accessed here (Please copy paste the total link in your browser address bar)

<https://www.sdiarticle5.com/review-history/107554>